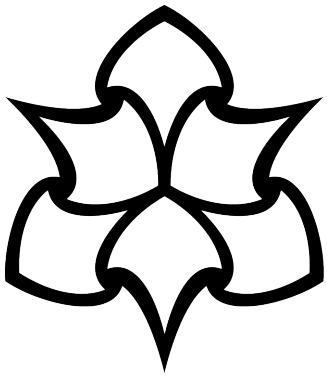

Journal of Colloid and Interface Science 622 (2022) 503–514

Contents lists available at ScienceDirect

Journal of Colloid and Interface Science

journal homepage: www.elsevier.com/locate/jcis

Multi-species colloidosomes by surface-modified lactic acid bacteria with enhanced aggregation properties

Xiaoyi Jiang [a], Helle Jakobe Martens [b], Elhamalsadat Shekarforoush [a], Musemma Kedir Muhammed [a], Kathryn A. Whitehead [c], Nils Arneborg [a], Jens Risbo [a,*]

[a] University of Copenhagen, Department of Food Science, Rolighedsvej 30, DK-1958 Copenhagen, Denmark
[b] University of Copenhagen, Department of Geosciences and Natural Resource Management, Rolighedsvej 23, DK-1958 Copenhagen, Denmark
[c] Manchester Metropolitan University, Department of Life Sciences, Chester St, Manchester M15GD, United Kingdom

GRAPHICAL ABSTRACT

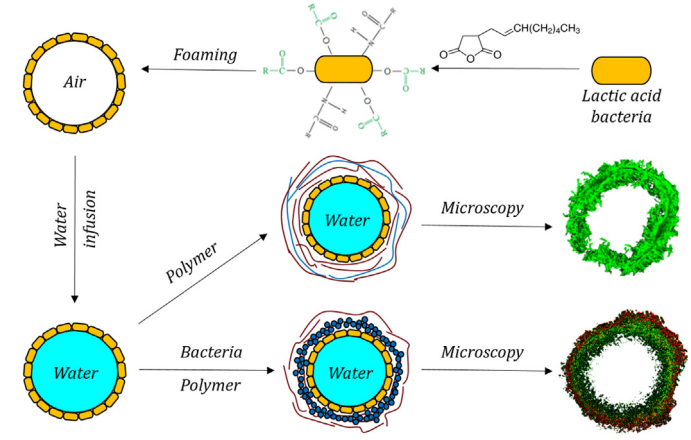

Stable colloidosome

ARTICLE INFO

Article history:
Received 21 January 2022
Revised 11 April 2022
Accepted 23 April 2022
Available online 29 April 2022

Keywords:
Colloidosome
Adsorption
Aggregation
Microbubbles
Layer-by-layer
Lactic acid bacteria
Octenyl succinic anhydride

ABSTRACT

Hypothesis: Surface modification of lactic acid bacteria enhances their adsorption and aggregation at air–water interface and enables stabilization of microbubbles that spontaneously transform into water-filled colloidosomes, which can be further modified using LBL formulations.
Experiments: The bacterial physicochemical properties were characterized using water contact angle (WCA) measurement, bacterial aggregation assay and zeta potential measurement. Cell viability was enumerated using plate-counting method. The LBL reinforcement of colloidosomes was examined by zeta potential measurement and the formed microstructure was investigated using bright-field microscopy, confocal laser scanning microscopy (CLSM) and scanning electron microscopy (SEM). Shell permeability of colloidosomes was evaluated using a dye release study.
Findings: Bacteria surface-modified using octenyl succinic anhydride (OSA) expressed strong adsorption and aggregation at air–water interface when producing microbubbles. Bacteria with enhanced aggregation ability formed stable shells, enabling complete removal of air and air–water interface without shell disintegration. The formed colloidosomes were studied as they were, or were further reinforced by LBL

* Corresponding author.
E-mail address: jri@food.ku.dk (J. Risbo).

https://doi.org/10.1016/j.jcis.2022.04.136

deposition using polymer or hybrid formulations. Hybrid coating involved assembly of two bacterial species producing colloidosomes with low shell porosity. The findings can be exploited to organize different living bacteria into structured materials and to encapsulate and release substances of diverse sizes and surface properties.

1. Introduction

Colloidosomes are hollow microcapsules with the shell being composed of densely-packed colloidal particles [1,2]. This kind of structure has recently received an increase in attention due to its potential to be used in the encapsulation and controlled release of fragile compounds for food, pharmaceutical, cosmetic and agricultural products [3]. The synthesis of colloidosomes most often requires the close self-assembly of colloidal particles onto an oil–water or air–water interface to form the so-called Pickering colloidal templates [4]. Typical particles used for preparing colloidosome templates are inorganic particles such as silica nanoparticles [5–7] and polystyrene latex [1,8,9]. The formed colloidal templates need further reinforcement such as thermal annealing [10,11], covalent crosslinking [12,13] or polymerization [14,15], to lock the particles together to be able to withstand the subsequent removal of internal phase.

Layer-by-layer (LBL) deposition of oppositely-charged materials via electrostatic adsorption is another route to physically reinforce colloidal templates [16–18]. Typical materials for LBL adsorption are polyelectrolytes such as poly(sodium styrenesulfonate) [5], poly(diallyldimethylammonium chloride) [19], pectin, as well as charged proteins [3]. In addition, modified silica nanoparticles are also used to define the porousness and thus the permeability of colloidosomes [3,5]. A previous report compared colloidosomes of polystyrene particles locked by either sintering or LBL electrostatic binding of poly-L-lysine, and found out that colloidosomes produced using the LBL method were more elastic and deformable, while sintering merely resulted in brittle colloidosomes [20]. Moreover, compared with other methods that normally involve heat treatment [2,21], reinforcement by LBL adsorption allows for a mild and non-invasive process which can be a huge advantage when dealing with colloidosomes based on biological building blocks.

Lactic acid bacteria, as uniformly micron-sized particles, are thus interesting candidates for the synthesis of colloidosomes. However, the surface properties of most lactic acid bacterial strains are dominantly hydrophilic, due to the large presence of peptidoglycan with a high ratio of polysaccharides to hydrocarbons [22,23]. These hydrophilic polysaccharides on the cell surface in other way provide steric repulsive forces between cells [24]. Chemical modification by covalently grafting hydrophobic moieties of small molecules onto a bacterial surface is a way to fine tune the cell hydrophobicity; such modified bacteria have been demonstrated to produce stable colloidal structures such as foams, emulsions [25] and double emulsions [26] via a Pickering mechanism. Compared to foams and emulsions, colloidosomes are more delicate structures. The only example of a colloidosome based on microorganisms was the so-called yeastosome which was formed via the adherence of polyelectrolyte-coated yeast cells to air–water interface via electrostatic attraction, followed by deposition of another layer of polyelectrolyte to lock the adsorbed cells together and prevent disintegration upon removal of the air–water interface [27].

This work aimed to tune the adsorption and aggregation properties of non-pathogenic lactic acid bacteria *Lactobacillus crispatus* (LBC) towards their efficient stabilization of microbubble templates for the preparation of colloidosomes, which were studied as it was or further modified via LBL electrostatic deposition using either polymers or polymer-bacteria hybrid formulations. The idea is that self-assembly and fast aggregation of LBC on air–water interface can be enabled by modifying the bacterial surface with octenyl succinic anhydride (OSA) in order to promote Pickering-driven adsorption by increasing air–water contact angle and limit the steric repulsion of the polysaccharide layer of the cell wall.

2. Material and methods

2.1. Materials and chemicals

Octenyl succinic anhydride (OSA), glycerol, dimethyl sulfoxide (DMSO), sodium chloride (NaCl), potassium chloride (KCl), disodium hydrogen phosphate (Na_2HPO_4), potassium dihydrogen phosphate (KH_2PO_4), 4′,6-Diamidino-2-phenylindole (DAPI), chitosan (extracted and/or purified from Pandalus borealis shell, low molecular weight, deacetylation $\geq$ 75%), anhydrous methanol, acetic acid (glacial, $\geq$99.85%), fluorescein sodium and FITC (Fluorescein 5(6)-isothiocyanate) were purchased from Sigma-Aldrich, Steinheim, Germany. Dextran sulfate sodium salt was purchased from Pharmacia Biotech, Uppsala, Sweden. Dialysis membrane tubing was obtained from Spectra/Por (MWCO: 12-14,000), CA, USA. SYTO 9 and NucRed™ Live 647 ReadyProbes™ Reagent were bought from ThermoFisher Scientific, Molecular Probes, Eugene, OR, USA. *Lactobacillus crispatus* DSM20584 (LBC) and *Pediococcus pentosaceus* strain 4412 (PCP) were kindly obtained from strain collection of Department of Food Science, University of Copenhagen (Finn Kvist Vogensen, Personal communication). MRS broth and agar (de Man, Rogosa and Sharpe) were bought from Oxoid, Basingstoke, England and atmosphere generation system (AnaeroGen sachets) was bought from Oxoid, Basingstoke, England. All the chemicals were used as received, except for MRS broth and agar which were sterilized in an autoclave (115 °C, 10 min) before use. MilliQ water (18.2 MΩcm at 25 °C, pH 5.6) was used in all the experiments.

2.2. Growth of bacteria and dry biomass determination

Lactobacillus crispatus DSM20584 (LBC) and *Pediococcus pentosaceus* strain 4412 (PCP) from frozen stock were anaerobically propagated (100 μL) in 10 mL MRS broth for 24 h. Then, 250 μL of the bacterial preculture was anaerobically incubated in 50 mL MRS broth at 37 °C and 30 °C for LBC and PCP, respectively. Finally, cells were collected from late exponential phase (16 h) by centrifugation at 5000 × g for 5 min at 4 °C, and LBC was washed twice with sterile MilliQ water while PCP was washed twice with 0.15 M NaCl (pH 5.6).

The dry weight of the bacterial cells was determined following a standard method [28]. Briefly, after growing for 24 h, cells were washed twice with either MilliQ water or 0.15 M NaCl (pH 5.6) passed through a 0.22 μm-pore-size cellulose membrane. The harvested cell pellets were re-suspended in 3 mL sterile MilliQ water. One milliliter cell suspension was transferred to a pre-weighed sterile aluminum boat. The bacteria were dried in a hot air oven

at 105 °C, and the total weight was measured regularly until a stable dry weight was obtained. The procedure was carried out in triplicate. The dry biomass corresponding to 250 μL preculture in 50 mL broth was 34.8 ± 0.5 mg for LBC and 30.7 ± 0.3 mg for PCP.

2.3. OSA modification of LBC bacteria

OSA modification of the LBC was adapted from a previous protocol [25]. Briefly, after 24-hour growth in 50 mL broth, bacteria were collected and washed twice with MilliQ water, the cell pellets were re-suspended in phosphate buffered saline (PBS), pH 7.4 with a final bacterial concentration of 0.35 wt%. The pH of bacterial suspension was standardized to 7.8 and different concentrations of OSA (3, 6, 10 w/w% based on the cell dry weight) in DMSO solution was slowly added into bacterial suspension while the pH of reaction was maintained between 7.4 and 7.8 by adding 0.1 M NaOH solution. The final concentration of DMSO in bacterial suspension was fixed at 2%. When the pH was constant for at least 15 min, the reaction was allowed to proceed for another 1 h. Finally, bacteria were harvested and washed twice by centrifugation at 5000 × g for 5 min at 4 °C.

2.4. Water contact angle measurements

Bacterial surface wettability was evaluated by water contact angle (WCA) measurements of bacterial lawns. First, unmodified and 3, 6, and 10 w/w% OSA-modified LBC were re-suspended in 50 mL 0.15 M NaCl (pH 5.6). The bacterial suspensions were passed through 0.45 μm pore size polyvinylidene difluoride membrane filters with the assistance of negative pressure. The filters deposited with a thick layer of bacterial lawn were carefully fixed onto normal glass slides using double-sided tapes and air-dried in a fume hood for approximately 90 min to enable the formation of the plateau contact angles [29]. The WCAs of bacteria were measured using the sessile drop method at room temperature with optical contact angle measuring and contour analysis systems (OCA 25, Dataphysics Instruments, Stuttgart, Germany). For each measurement, at least three filters were prepared, and five water droplets of 3 μL were dispensed on the same filter in different dried areas.

2.5. Bacterial aggregation assay

The bacterial aggregation (in microbiology often termed "autoaggregation") was investigated according to a previous method [30] with minor modifications. Briefly, unmodified and OSA-modified LBC bacteria collected from 50 mL MRS broth were washed twice with MilliQ water and re-suspended in PBS (pH 7.2). The OD of the bacterial suspension was adjusted to 1.0 at 600 nm, which corresponded to a cell concentration of 2×10^8 CFU/mL. After standing for certain time intervals (0, 1, 2, 3, 5 h) at room temperature, the upper part of bacterial suspension (around 0.5 cm below the liquid level) was carefully transferred without disturbing the lower bacterial suspension to measure OD at 600 nm. The kinetics of bacterial sedimentation termed as aggregation coefficient (ACt) was calculated based on the equation,

$$ACt = \left(1 - \frac{A_t}{A_i}\right) \times 100 \quad (1)$$

where A_i represents the initial OD of the bacterial suspension at 600 nm and A_t is the OD600 of upper part of bacterial suspension at time t. All results were obtained from duplicated experiments and data are presented as average ± standard error.

2.6. Zeta potential measurements

The surface charge of unmodified and OSA-modified LBC was measured using a zeta sizer (Malvern Zetasizer, Nano ZSP, UK). All the measurements were conducted at 25 °C using MilliQ water as the background electrolyte solution. Unmodified and modified cell pellets were suspended in 20 mL MilliQ. The suspension was diluted 10 times and 1 mL of the diluted suspension was injected into a folded capillary cell using a disposable syringe. Before each measurement, the capillary cell was rinsed by subsequently flushing through ethanol, MilliQ water and the sample. All the data reported are the averages of duplicates and the results are presented as average ± standard error.

2.7. Enumeration of bacterial viability

The viability of LBC bacteria before and after OSA modification was investigated by using the plate counting method. Briefly, cell pellets with and without modification were suspended in 50 mL sterile MilliQ water. After preparing the serial dilutions, 30 μL of each dilution was evenly distributed in 6 to 7 drops on one quarter of an MRS agar plate and all the plates were incubated anaerobically at 37 °C for at least 48 h. After the formation of visible colonies, only dilutions with number of appeared colonies between 30 and 300 were selected for counting. The count for culturable bacteria in each suspension was expressed in colony forming units per milliliter (CFU/mL). The viability test was carried out for unmodified and 3, 6, 10 w/w% OSA-modified LBC immediately after modification. All the data are presented as average ± standard error from duplicated experiments.

2.8. Preparation of coating materials

For chitosan (CH) solution, 1% glacial acetic acid in 0.15 M NaCl solution was prepared and the pH was adjusted to 5.6 before dissolving the chitosan (0.75 mg/mL). The mixture was stirred for 12 h at room temperature to allow the complete dissolution of the CH. Before use, the CH solution was centrifuged at 5000 × g for 10 min and the supernatant was filtered through a 0.22 μm-pore-size cellulose membrane. The preparation of dextran sulfate (DS) solution was obtained by dissolving dextran sulfate sodium salt (0.75 mg/mL) into MilliQ water. The PCP suspensions were prepared by adding 1 mg/mL (based on dry biomass) of PCP cells into 0.15 M NaCl (pH 5.6).

The preparation of fluorescent chitosan for microscopic investigation was adapted from a previous report [31]. Briefly, 1 g of chitosan was dissolved in 100 mL of 1% acetic acid overnight. To this CH solution, 100 mL of anhydrous methanol was added under continuous stirring. Then, 50 mL of FITC solution in methanol (1 mg/mL) was slowly added and the reaction was allowed to proceed in darkness for 3 h at room temperature. After the reaction had completed, FITC-labeled chitosan was precipitated using 0.5 M NaOH, and the precipitate was collected and washed in methanol: water (70:30 v/v) by centrifugation at 5000 × g for 10 min. The centrifugation/washing cycle was repeated until no free FITC fluorescence was detected in the supernatant using fluorescence microscopy. Finally, the FITC-labeled chitosan was extensively dialyzed against deionized water in darkness for 3 days and freeze-dried.

2.9. Preparation and LBL coating of air bubble-templated colloidosomes

The preparation of colloidosomes including template microbubble creation and layer-by-layer (LBL) coating is schematically illustrated (Fig. 1). Unmodified and different degrees of OSA-modified

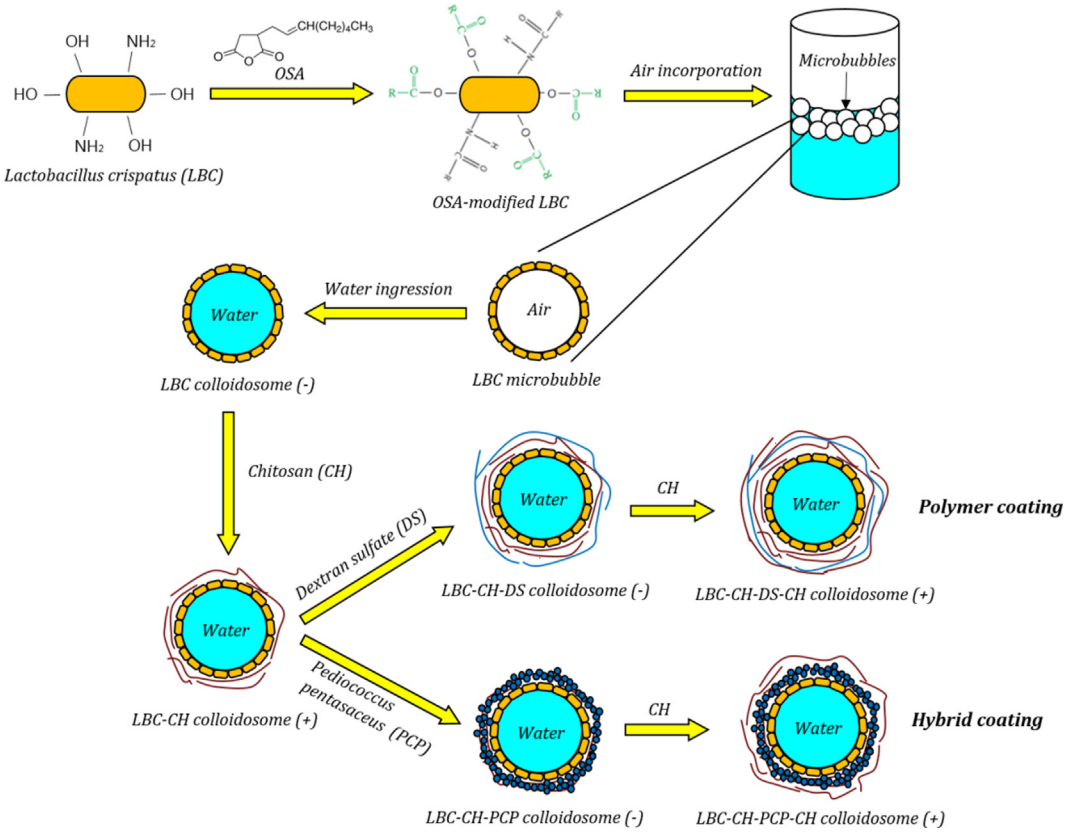

Fig. 1. Schematic preparation of water-filled colloidosomes by transformation of microbubbles stabilized by OSA-modified *Lactobacillus crispatus* (LBC). Different formulations exist for the colloidosomes. The simplest "LBC colloidosome" is made using LBC which is stable in itself and can be further coated by chitosan to obtain "LBC-CH colloidosome". Further reinforcement is done using either polymer or hybrid coating formulations depending on the use of either anionic DS or the negatively-charged bacterial cells of *Pediococcus pentosaceus* (PCP). The formed "LBC-CH-DS colloidosome" and "LBC-CH-PCP colloidosome" can be finished by the outermost layer of CH. The sign of the surface charge of each formulation is indicated in parenthesis.

LBC cells were collected and re-suspended in 3 mL 0.15 M NaCl (pH 5.6) in a 15-mL centrifuge tube. After 10 min equilibration at room temperature, air was incorporated by vigorously hand shaking for 30 s to produce microbubbles. The microbubbles adsorbed by cells were let to stand at room temperature for at least 16 h, during which time the air core of the microbubbles was gradually substituted with the ambient aqueous NaCl solution and finally the heavier water-core colloidosomes were gravitationally settled down to the bottom after over-night standing. The complete sedimentation of colloidosomes was confirmed by bright-field microscopy that only free bacteria were present in the supernatant. Finally, the colloidosomes were washed off the free bacteria by replacing the supernatant with 0.15 M NaCl (pH 5.6) thrice. The prepared colloidosomes were thereafter denoted as LBC colloidosomes.

The LBC colloidosomes prepared using 10 w/w% OSA-modified LBC were electrostatically coated using LBL-based procedure according to a previously-reported protocol with some modifications [5]. Briefly, 0.5 mL LBC colloidosome pellets were re-suspended in 10 mL CH solution, and this mixture was shaken on a rotator at 60 rpm for 20 min. After complete sedimentation of CH-coated colloidosomes assisted with mild centrifugation at 500 × g for 2 min, the colloidosomes were washed twice using NaCl solution (0.15 M, pH 5.6). After the adsorption of first CH layer, the next negatively-charged DS layer was deposited following the same procedure as described above. Alternatively, the second layer was added by PCP cells, which was performed by re-suspending CH-coated colloidosomes in 10 mL PCP suspension in 0.15 M NaCl (pH 5.6) followed by the same mixing and washing procedures. An outermost layer of CH was deposited as described above. Finally, the different formulations of colloidosomes were stored in 0.15 M NaCl (pH 5.6) at room temperature until further investigation. Formulations involving only polymers (CH and DS) were denoted as polymer coating, while formulations combining CH and PCP bacteria are denoted as hybrid coatings.

2.10. Characterization of colloidosomes

2.10.1. Surface charge

The zeta potential of colloidosomes was investigated using a zeta sizer at 25 °C (Malvern Zetasizer, Nano ZSP, UK). For the measurement, the samples were prepared by re-suspending colloidosomes corresponding to 250 μL preculture in 50 mL broth in 8 mL MilliQ water (pH 5.6). All the data reported are the averages of duplicates and the results are presented as average ± standard error.

2.10.2. Bright-field microscopy

All the images were captured by a Cool Snap RS Photometrics camera (Roper Scientific, Tucson, AZ, USA) connected to Zeiss Axioskop microscope (Carl Zeiss, Goet- tingen, Germany), and processed with ImageJ software. Bright-field microscopy was applied to study the microstructure of LBC colloidosomes. First, LBC colloidosomes prepared using different OSA concentrations (3, 6, 10 w/w %) were washed thrice using 0.15 M NaCl (pH 5.6) and the "clean" LBC colloidosomes were observed at 100 × magnification. In addition, to study the gradual infusion of aqueous phase into the microbubbles, microbubbles prepared using 10 w/w% OSA-modified LBC were taken at 0, 5 and 10 min, respectively, after

microbubble generation and observed at magnifications of 100 × and 400 ×.

2.10.3. Confocal laser scanning microscopy

A confocal laser scanning microscope (Point Scanning Confocal and 2-photon microscope SP5-X MP UV, Leica Microsystems, Germany) was used to investigate the location of outermost CH layer in polymer coating, and the location of two bacterial layers in hybrid coating. In the observation of CH location, the FITC-labeled CH was used as the outermost coating layer. For investigation of double bacterial layers, the inner LBC layer was stained using SYTO 9 and the outer PCP layer was stained by NucRed™ Live 647 ReadyProbes™ Reagent. For the staining of LBC, cells for microbubble generation were suspended in 1 mL 0.15 M NaCl (pH 5.6) and 2 μL SYTO 9 solution (3.34 mM in DMSO) was added. After 15 min incubation in the darkness at room temperature, cells were washed twice and re-suspended in 3 mL 0.15 M NaCl (pH 5.6) for microbubble preparation. In the staining of PCP coating layer, 2 drops of NucRed™ Live 647 ReadyProbes™ Reagent were added to 1 mL cell suspension, followed by the incubation and washing procedure stated above. All the samples were observed at 630 × magnification within 10 min after sample preparation to avoid moisture evaporation. For the investigation of polymer coating, XYZ scanning was performed in an average of 6 lines and the resolution of the final images was 0.28 μm/0.28 μm/0.98 μm for X, Y and Z dimension, respectively. In the study of hybrid coating, XY scanning was employed in an average of 8 lines and the resolution of the final images was 0.26 μm/0.26 μm for X and Y dimension, respectively. The images were processed by Leica Microsystems LAS AL lite software (Germany).

2.10.4. Scanning electron microscopy (SEM)

SEM was utilized to investigate the microstructure of the polymer and hybrid surface coated colloidosomes. The colloidosomes were fixed in 2.5% glutaraldehyde in 0.1 M cacodylate buffer, at pH 7.3, 5 °C for 2 h. Then, samples were subsequently rinsed in the same buffer and water each for 10 min and dehydrated in a graded ethanol series (50, 70, 90, 95, 100%) for 10 min. Finally, samples were dried in hexamethyldisilazane (HMDS, trimethylsilylamine) for 30 min and the dried samples were spread onto a filter paper and left overnight before being mounted onto metal stubs with double-sided carbon tape. Samples were sputter-coated with a thin layer of gold under vacuum, using an automated sputter coater (Leica Coater ACE 200, Wetzlar, Germany). Imaging was carried out using a FEI Quanta 3D FEG scanning electron microscope operating at 2.00 kV and 10.000 × to 100.000× magnification. Contrast adjustments were carried out using Adobe Photoshop CS5 (USA).

2.11. Dye release study

The study on fluorescent dye release was adapted from work by others [8]. Briefly, colloidosomes of different coating formulations were suspended in 3 mL 0.15 M NaCl solution (pH 5.6). To this suspension, 30 μL fluorescein sodium solution (1 μg/mL) was added and the mixture was incubated in darkness at room temperature for 3 days. The equilibrium of dye diffusion was driven by concentration difference between the inside and outside of a colloidosome, and therefore long-time incubation enabled the identical amount of fluorescein sodium dye encapsulated within all the colloidosomes (0.01 μg/mL). After gravitational settling of dye-loaded colloidosomes, the dyed supernatant was removed and 30 mL MilliQ water was added, which initiated the release of encapsulated dye under continuous stirring for 30 min. At certain time intervals, 1 mL dyed suspension was filtered through a 0.22 μm-pore-size cellulose membrane to measure the absorbance using a spectrophotometer (Evolution™ 350 UV–Vis Spectrophotometer, Thermo Scientific, Waltham, MA, USA) at 495 nm. The dye release (%) was calculated from the following equation,

$$\text{Dye release}\,(\%) = \frac{A_t - A_0}{A_1 - A_0} \times 100 \quad (2)$$

where A_0 and A_1 refer to the absorbance at time 0 min and the absorbance after complete release of encapsulated dye, respectively, and A_t represents the absorbance at time interval t min. The normalized percentages of dye release (y) at several time intervals (0–5, 8, 10, 15, 20, 25, 30 min) were regressed with a function of the form,

$$y = 1 - e^{-bt} \quad (3)$$

where b is a measure of the rate of equilibration. All results were obtained from duplicated experiments and data are presented as average ± standard error.

3. Results and discussion

3.1. Characterization of LBC after OSA modification

Based on the complexity of bacterial cells, OSA can react with both hydroxyl groups and amine groups located in either the cell wall or the interior of bacteria, which makes the accurate quantification of grafted OSA molecules somewhat difficult. Despite these difficulties, notable changes were still induced by OSA modification in terms of bacterial viability and surface properties including wettability and zeta potential (Table 1).

The alteration of surface physicochemical properties by OSA modification might accompany some effects on bacterial viability. Indeed, results of measurements of culturability (reported as log CFU/mL in Table 1) demonstrated a negative effect of OSA modification on the viability of LBC and this effect was strongly dose-dependent. Generally, all the OSA-modified bacteria experienced an evident drop in colony formation ability compared to unmodified bacteria, with 10 w/w% OSA concentration inducing the strongest culturability reduction from 8.3 log to 5.5 log CFU/mL. These results were in agreement with the information obtained from cell integrity investigations using fluorescence microscopy, where most severe damage in cell membrane intactness was found for 10 w/w% OSA modification (Fig. S4). It could be therefore inferred that a stronger response in surface wettability by OSA modification also induced a more detrimental effect on the cell viability. However, based on applications towards different purposes, a balance between desired surface properties and bacterial viability could be accessed by differently dosing the OSA concentration.

The stabilization of Pickering-stabilized microbubbles needs a high packing density of bacteria on air–water interface [32], which in turn requires the minimization or elimination of electrostatic repulsion between bacteria by neutralizing the surface charge. After OSA modification, there was only a minor decrease of negative surface charges from −50.5 to −43.4 mV even with 10 w/w% OSA concentration (Table 1), indicating slightly reduced but still strong electrostatic repulsions between bacterial cells. The slight change in surface negative charges was most likely affected by the shift of slipping plane due to the attachment of multiple hydrophobic chains. In view of this, medium of high ionic strength (150 mM NaCl) was utilized when producing microbubbles to screen the electrostatic interactions between cells and favor a dense packing of bacteria on the air–water interface.

Pickering stabilization of air bubbles greatly depends on the water contact angle of bacteria which is related to cell wettability [4]. To favor the bacterial adsorption onto the interface, the wettability of the cells needs to be modified to a WCA (θ) in the vicinity

Table 1
Characterization of unmodified and OSA-modified bacteria in terms of WCA, zeta potential and culturability in log CFU/mL.

OSA conc. (w/w%)	WCA (θ, degree)	$(1-\|\cos\theta\|)^2$	Zeta potential (mV)	Viability (log CFU/mL)
0	75 (2)	0.5 (0.1)	−50.5 (1.7)	8.3 (0.1)
3	93 (4)	0.8 (0.1)	−48.2 (1.7)	6.4 (0.0)
6	104 (3)	0.6 (0.1)	−46.7 (0.4)	5.9 (0.1)
10	107 (2)	0.5 (0.1)	−43.4 (1.2)	5.5 (0.1)

Values are represented as mean values resulted from duplicated experiments. Standard error is given in parentheses.

of 90° so the desorption energy reaches the maximum [33]. The WCAs of unmodified and 3, 6, 10 w/w% OSA-modified LBC are listed in Table 1. Compared to most *Lactobacillus* strains which normally showed a θ below 70° [34,35], unmodified LBC exhibited a somewhat high θ of 75°. OSA modification increased the WCA as a function of OSA dosage, and the highest modification of 10 w/w% gave the highest θ of 107°. This confirmed the effectiveness of OSA modification on grafting aliphatic chains onto bacterial surface and lowering the cell wettability. The desorption energy of Pickering particles from the air–water interface is proportional to a factor of $(1-|\cos\theta|)^2$ [36], and this factor is also reported in Table 1. Compared to unmodified LBC, mild modifications with 3 and 6 w/w% OSA led to a 1.6- and 1.2-fold increase in $(1-|\cos\theta|)^2$, respectively, indicating only a slight improvement of bacterial desorption energy by OSA modification. For micron-sized particles at air–water interface, the order of magnitude of the desorption energy is approx. 10^7 kT and this indicates that even unmodified LBC should be able to adsorb and bind irreversibly at the interface, and the minor changes in the measured θ induced by chemical modification might not in itself be decisive for the Pickering effect of bacteria. Here, it should be mentioned that the hydrated surface of bacteria is polymeric and flexible, and drying process prior to WCA measurement might cause the collapse of polymeric surface and expose some hydrophobic components, thus not fully capturing the modified steric repulsions that were originally rendered by hydrophilic polymers.

Bacterial aggregation (also called autoaggregation) was studied by monitoring cell sedimentation over 5 h (Fig. 2). First, unmodified LBC already showed some degrees of aggregation with around 26% of the total cells sedimenting in first-hour incubation, which was comparatively higher than the typical values below 15% reported for other *Lactobacillus* species [30,37]. After OSA modification, the sedimentation was considerably faster, where above 50% cells sedimented within 1 h with 6 and 10 w/w% OSA modification. In comparison, 3 w/w% OSA modification resulted in slower aggregation than highly-modified bacteria but notably faster aggregation than unmodified bacteria. However, no obvious difference was observed between 6 and 10 w/w% OSA-modified bacteria within the experimental accuracy.

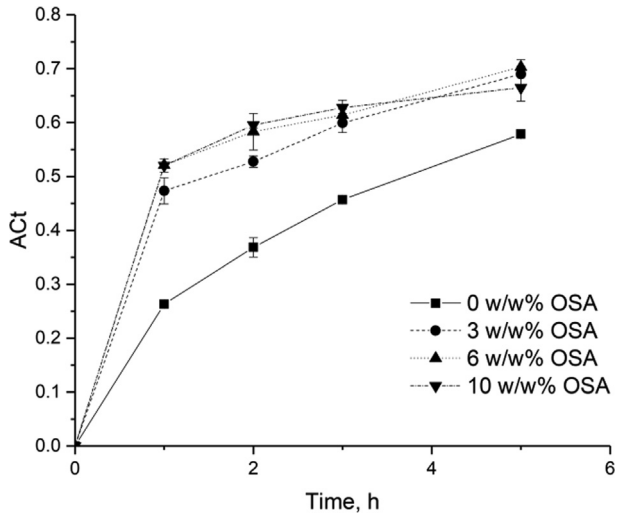

Fig. 2. Bacterial aggregation as evaluated by sedimentation of unmodified, 3, 6 and 10 w/w% OSA-modified LBC bacteria. Error bars represent the standard errors.

According to the theory of colloidal stability, aggregation of colloidal particles like bacteria should result from the reduction or elimination of fundamental repulsive forces including steric and electrostatic repulsions. Here, the electrostatic effect was seemingly not the cause of the changed repulsion, since only a small change in zeta potential after OSA modification was observed, which was further screened by the use of high ionic strength. Therefore, aggregation in aqueous solution was more likely triggered by the loss of steric repulsion originally provided by hydrophilic polymers such as cell wall cross-linked polysaccharides [24], which were also targeted by OSA modification. A mechanism of action for this scenario could be that the aqueous compatibility of the polysaccharides with water was lost upon grafting of the hydrophobic chains, resulting in the polymeric layers collapsing on the bacterial surface with the consequence of loss of steric repulsion. Again, these changes in the surface "hairiness" or "fuzziness" cannot be captured by WCA measurement and their investigation can be however difficult, as any pretreatment inevitably affects the mobility and structure of the surface polymeric components. Therefore, efforts could be made in the future to develop surface-sensitive techniques for microorganisms to allow the non-destructive analysis of cell surface conformation under their natural (e.g. fully-hydrated) state.

3.2. Formation of microbubbles and microstructure of the resulting colloidosomes

Air was incorporated by handshaking. For unmodified LBC, a stable foam of coarse bubbles was generated on top of a highly turbid suspension (Fig. 3a), indicating lack of generation of microbubbles and a high degree of untrapped free bacteria in the aqueous phase. On the contrary, for modified bacteria, air incorporation resulted in a layer of fine foam on top of a clearer aqueous phase, indicating smaller air bubbles that were able to trap a larger proportion of bacteria. This confirmed that the chemical modification enhanced the adsorption of LBC despite the modest changes of the observed WCA.

Most microbubbles of the fine foam generated by modified LBC were able to transform spontaneously into water-filled colloidosomes within 10 min. The colloidosomes were visualized using bright-field microscopy after washing away the non-adsorbed cells (Fig. 3b-d). This revealed colloidosomes with a size range of 20 to 70 μm independent of the degree of bacterial modification, in agreement with the quantitative results from particle size distributions and mean diameter analyses (Fig. S1 and Table S1). Instead, the main differences among 3, 6 and 10 w/w% OSA modifications were found in the number of free cells remained after washing as well as the bacterial packing density of formed LBC colloidosomes. Compared to LBC colloidosomes prepared with highly-modified LBC (Fig. 3c, d), samples with 3 w/w% OSA modification

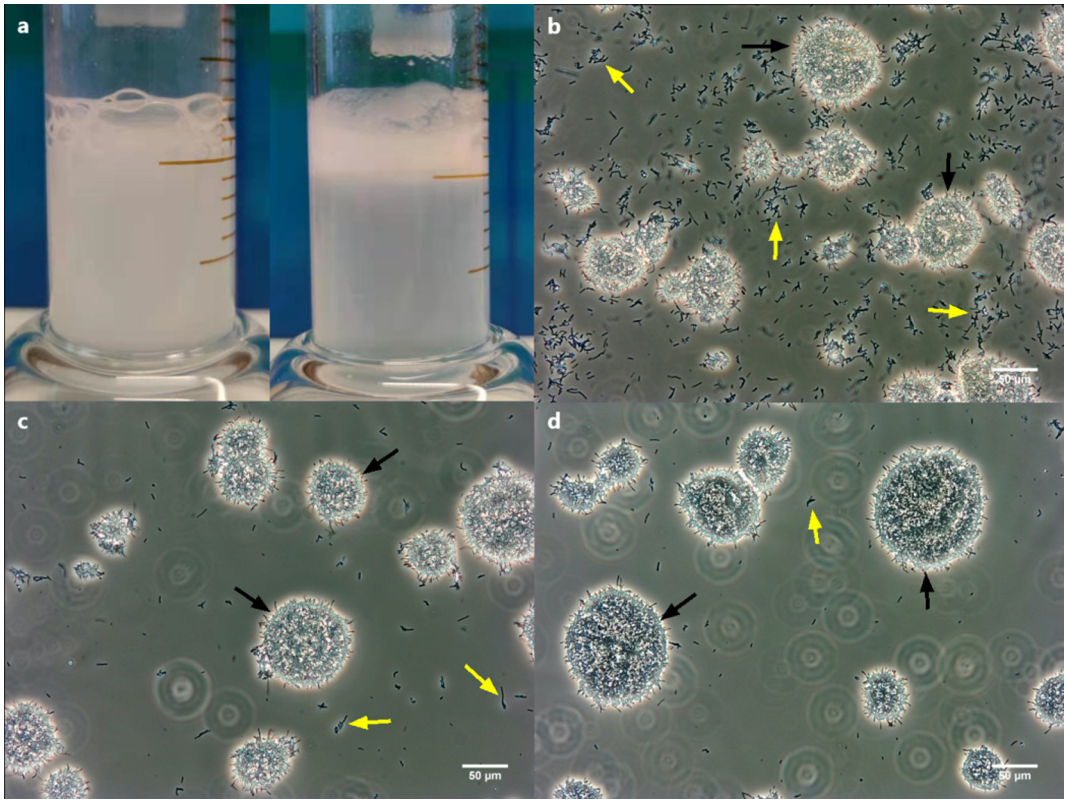

Fig. 3. (a) Foam generated from suspensions of unmodified (left) and 10 w/w% OSA-modified (right) bacteria in 0.15 M NaCl solution. LBC colloidosomes prepared with 3 (b), 6 (c) and 10 (d) w/w% OSA-modified bacteria showing the different amount of free cells in the aqueous phase after washing away the non-adsorbed bacteria. Black and yellow arrows indicate the water-core LBC colloidosomes and free bacteria, respectively. Scale bars represent 50 µm.

contained a large amount of free bacteria in the aqueous compartment even after washing three times (Fig. 3b). In contrast, the use of 10 w/w% OSA-modified bacteria resulted in LBC colloidosomes with higher bacterial packing density than especially 3 w/w% OSA-modified bacteria, where cells packed rather loosely in the formed structures. Even though the bacterial packing density resulting from their aggregation ability seemed to influence the sizes of LBC colloidosomes by changing the wall thickness (Fig. S1 and Table S1), it was still difficult to precisely control the overall size of LBC colloidosomes as it primarily relied on the initial size of microbubble templates that was in turn affected by shaking process.

The observed free bacteria after washing resulted from the continuous release of bacteria from shells of formed LBC colloidosomes due to the weak binding and aggregation between adjacent cells. Therefore, the degree of non-adsorbed cells in the aqueous phase should go hand in hand with the bacterial packing density of the formed colloidosomes. Indeed, structures with most bacterial packing and aqueous phase with least untrapped bacteria were both observed after 10 w/w% OSA modification compared to mild modifications. This can be explained by the strongest bacterial aggregation ability after 10 w/w% OSA modification, probably owing to the most reduced steric repulsions between cells that were originally provided by wall polysaccharides. In view of this, only LBC colloidosomes of 10 w/w% OSA-modified bacteria were selected for further investigations and coating procedures.

In the early stages of colloidosome formation, the air–water exchange in the microbubbles was observed within 1, 5 and 10 min after foam generation (Fig. 4). Samples immediately after air incorporation consisted of mostly microbubbles fully covered by bacteria and only a few spherical air-free particles were present (Fig. 4a), that had converted very quickly before observation. In a micrograph with higher magnification (Fig. 4d), an air bubble was found to be covered by rod-shape bacteria that densely packed on the air–water interface. After standing for 5 min (Fig. 4b and 4e), the air phase started to shrink, revealing the partial exchange of air core by water. After 10 min, more complete ingression of water occurred (Fig. 4c) and the coexistence of a finished water-core LBC colloidosome and an air-core microbubble was observed (Fig. 4f).

During the observation process, faster air–water exchange always occurred with microbubbles of smaller sizes as small bubbles generates higher Laplace pressure that acts as a driving force towards Ostwald ripening [38,39], which in our case, is also most likely the main mechanism behind the air displacement when exchanging with water. This replacement by water core should in principle result in the eventual collapse of formed structure due to disappearance of the air–water interface and thus the Pickering effect [40]. In this case, however, alongside the irreversible adsorption rendered by high WCAs of bacteria, the promoted aggregation by OSA modification ensured the fast mutual locking of bacteria thus preventing the disintegration of structure. During air–water exchange, the air–water interface gradually detached from the colloidosome wall instead of causing bubble shrinkage or creating a facetted Ostwald-stable armored bubble [40–42]. The effect possibly relied on the stiffness of the thick wall of micron-sized bacteria instead of smaller nano-sized Pickering particles used for armored bubbles. Also because of this, possibilities existed that small air cavities might be formed in the interior of colloidosome shells due to random aggregation of rod-shaped LBC bacteria, eventually causing incomplete water ingression in the entire colloidosomes during air–water exchange.

In the only previous example of colloidosomes prepared from microorganism-stabilized microbubbles, the so-called

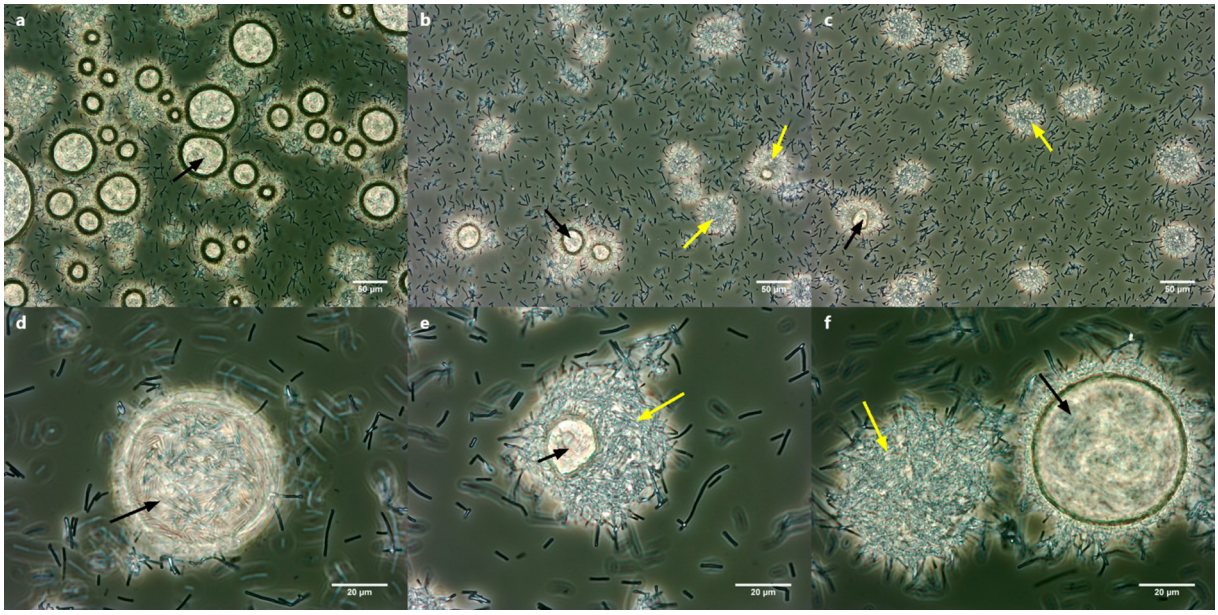

Fig. 4. Foam from suspensions of 10 w/w% OSA-modified bacteria in 0.15 M NaCl solution after 1 (a, d), 5 (b, e) and 10 (c, f) min preparation (free cells were unwashed). Gradual transformation of the microbubbles into water-core colloidosomes was observed (a-c). The air core of a microbubble (d) was partially infused with water (e) and eventually disappeared, which was in coexistence with another untransformed microbubble (f). Black and yellow arrows indicate the air core and water core, respectively. Scale bars represent 50 µm for a, b, c and 20 µm for d, e, f.

yeastosomes, the microbubbles were produced via electrostatic binding of poly(allylamine hydrochloride)-coated yeasts to oppositely charged air–water interface, and the formed templates needed to be reinforced by electrostatically depositing another layer of polyelectrolyte to stabilize the structure prior to air–water exchange [27]. The present work is based on a simpler principle involving only bacterial cells capable of adsorbing and aggregating on the air–water interface forming solid stable shells without stabilization from additional adsorption of polymers or polyelectrolytes.

3.3. Reinforcement of LBC colloidosomes by LBL deposition

The modification of colloidosomes was further achieved by LBL deposition of either polymers or bacterial cells onto the naked LBC colloidosomes. The information on the different formulations used to coat the colloidosomes was summarized (Table 2). Here, the LBL adsorption by polymers requires a polymer concentration just below the occurrence of depletion flocculation, but sufficient to cover the previous surface as much as possible [43,44]. Based on results from zeta potential measurement and bright-filed microscopy (Figs. S2 and S3), the polymer and bacterial concentration of 0.75 and 1 mg/mL, respectively, were chosen as the coating saturation effect was observed and no severe aggregation of colloidosomes occurred after washing away the excessive coating materials.

The coating of each layer was confirmed by measuring the net surface charge of colloidosomes. The naked LBC colloidosomes exhibited a negatively-charged surface of −37.6 mV, indicating the anionic surface possessed by OSA-modified LBC cells. The deposition of first CH layer brought the zeta potential to a positive side of +31.6 mV and a subsequent charge reversal always happened upon the addition of an oppositely-charged layer, regardless if polymer- or hybrid-coating formulations were used. Notably, the deposition of outermost CH layer resulted in a similar zeta potential to the first CH layer coating, which suggested a complete coverage of CH on the surface.

CLSM was utilized to study the location of specific coating layers such as CH and PCP. In the study of polymer coating including LBC-CH* and LBC-CH-DS-CH* colloidosomes, where the asterisk indicates fluorescence-labelled coating layer, a Z-stack series consisting of 15 sections was used to show the overall location of labelled chitosan on the surface of the colloidosomes (Fig. 5a and b). As can be seen, the CH* in LBC-CH* colloidosomes was deposited onto the individual LBC cells of negative charges, so the green fluorescence mainly came from the LBC cells coated with CH* and locations with low bacterial packing density were seen in darkness (Fig. 5a). In comparison, on the LBC-CH-DS-CH* colloidosomes, the outermost CH* displayed a more even coating and distribution on the entire colloidosome, and the inner LBC cells became nearly invisible due to the bright greenish fluorescence coming from the outer CH layer (Fig. 5b). An equatorial focus plane from a Z-stack

Table 2
Summarized information regarding colloidosomes fabricated using different Layer-by-layer coating formulations.

Sample number	Colloidosome formulation	Number of coating layer	Coating type	Zeta potential (mV)
1	LBC	0	None	−37.6 (1.9)
2	LBC-CH	1	Polymer	+31.6 (1.5)
3	LBC-CH-DS	2	Polymer	−12.0 (0.9)
4	LBC-CH-PCP	2	Hybrid	−25.6 (1.1)
5	LBC-CH-DS-CH	3	Polymer	+32.9 (0.8)
6	LBC-CH-PCP-CH	3	Hybrid	+32.2 (0.9)

Zeta potentials are represented as mean values resulted from duplicated experiments. Standard error is given in parentheses.

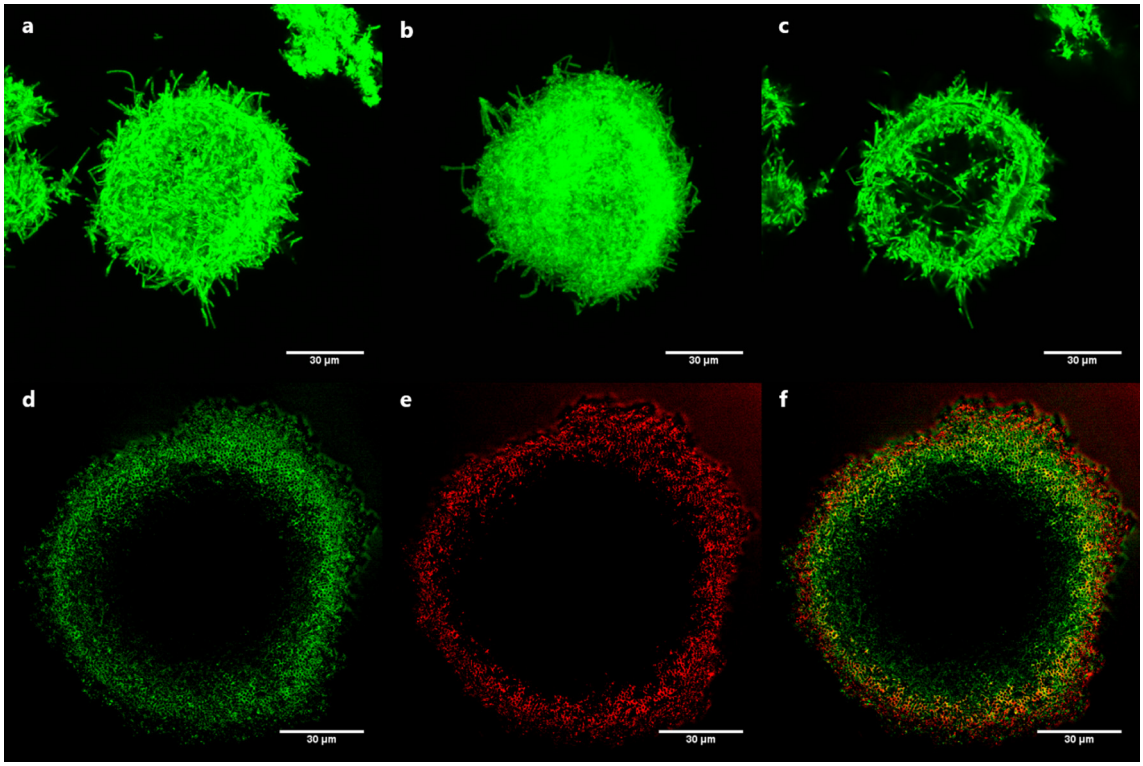

Fig. 5. LBC-CH* colloidosome (a) and LBC-CH-DS-CH* colloidosome (b) with the outermost CH layer labelled using FITC (green) showing different coating patterns of the outermost CH in the two formulations. The maximum intensity projections of a z-stack series of 15 image planes represented a total thickness of 14.69 μm of the sample. (c) The equatorial focal plane of LBC-CH colloidosome showing the hollow structure. The equatorial focal plane of hybrid-coated LBC*–CH-PCP*–CH colloidosome with the inner LBC layer labelled using SYTO 9 (green) (d) and outer PCP layer labelled using Nucred (red) (e). Merged channel shows complete coverage of the inner LBC layer by outer PCP layer (f). Scale bars represent 30 μm.

combination demonstrated the hollow structure of colloidosome (Fig. 5c).

The hollow structure was also confirmed for colloidosomes coated using hybrid formulations (Fig. 5d-f), demonstrating the equatorial ring of a LBC*–CH-PCP*–CH colloidosome using fluorescent labeling of the bacteria. The green fluorescence was emitted by the inner LBC cells stained with STYO 9 (Fig. 5d) and the outer PCP cells was differentiated by the red fluorescence of the Nucred stain (Fig. 5e). Both stains were cell-permeant and bound to cellular nucleic acids [45,46]. The combined channel of inner and outer bacteria suggested the deposition of an outer layer of PCP cells on the innermost LBC cells (Fig. 5f). The yellow fluorescence appearing in between the two layers indicated overlapped regions where the outer PCP bacteria were likely filling the interstitial space formed between the inner LBC cells.

3.4. Shell porosity and permeability of fabricated colloidosomes

The microstructure of polymer- and hybrid-coated colloidosomes was investigated using SEM and the micrographs of LBC-CH-DS-CH and LBC-CH-PCP-CH colloidosomes were demonstrated (Fig. 6). For polymer-coated colloidosomes (Fig. 6a), the overall spherical shape of microbubbles was well maintained after the removal of air-core templates and polymers were observed on bacterial surface, occasionally connecting the extended cells. A typically "hairy" surface was observed for the polymer-coated colloidosomes because the rod-shaped innermost LBC might show random packing and aggregation with either their transverse or longitudinal sections attaching to the air–water interface. In comparison, the outer surface of colloidosomes using the hybrid coating seemed to produce less 'hairy' features, probably due to the filling up of interstitial space by smaller-sized and round-shaped PCP bacteria (Fig. 6b). Moreover, some fractured colloidosomes accidentally exposed the inner structure, as shown by arrows (Fig. 6c and d). Unlike the irregular outer shape exhibited by all the colloidosomes, on the inner side, it appeared to be that the hairy-like projections had organized to produce a more smoothly spherical surface due to the densely packed LBC cells, which suggested the location of the original air–water interface before displacing the air core. For hybrid-coated LBC-CH-PCP-CH colloidosomes (Fig. 6d), the round-shaped PCP bacteria were observed not only depositing on the surface, but also filling up the open voids all the way through the wall of colloidosomes. As a consequence, hybrid coating involving PCP cells might result in colloidosomes with lower shell porosity than colloidosomes formulated only with polymers.

To investigate the shell permeability, colloidosomes formulated with different coating combinations were studied in terms of their release profiles of encapsulated fluorescein sodium dye. The normalized percentages of dye release at several time intervals were plotted and regressed (Fig. 7a). Generally, a good fitting of the dye release profiles was obtained for all the fabricated colloidosomes using an exponential function, which complied well with another drug release study fitted with the same model [47]. According to the first-order kinetics, all the colloidosomes presented a quick release behavior where the encapsulated dye was completely released after 30 min. Besides, the correlation between the colloidosome surface charge and constant b was demonstrated (Fig. 7b). Within group I, constituted by colloidosomes with maximum two coating layers, LBC, LBC-CH-PCP, LBC-CH-DS and LBC-CH, the permeability (as expressed by the parameter b) was linearly correlated with the zeta potential of the colloidosomes, indicating

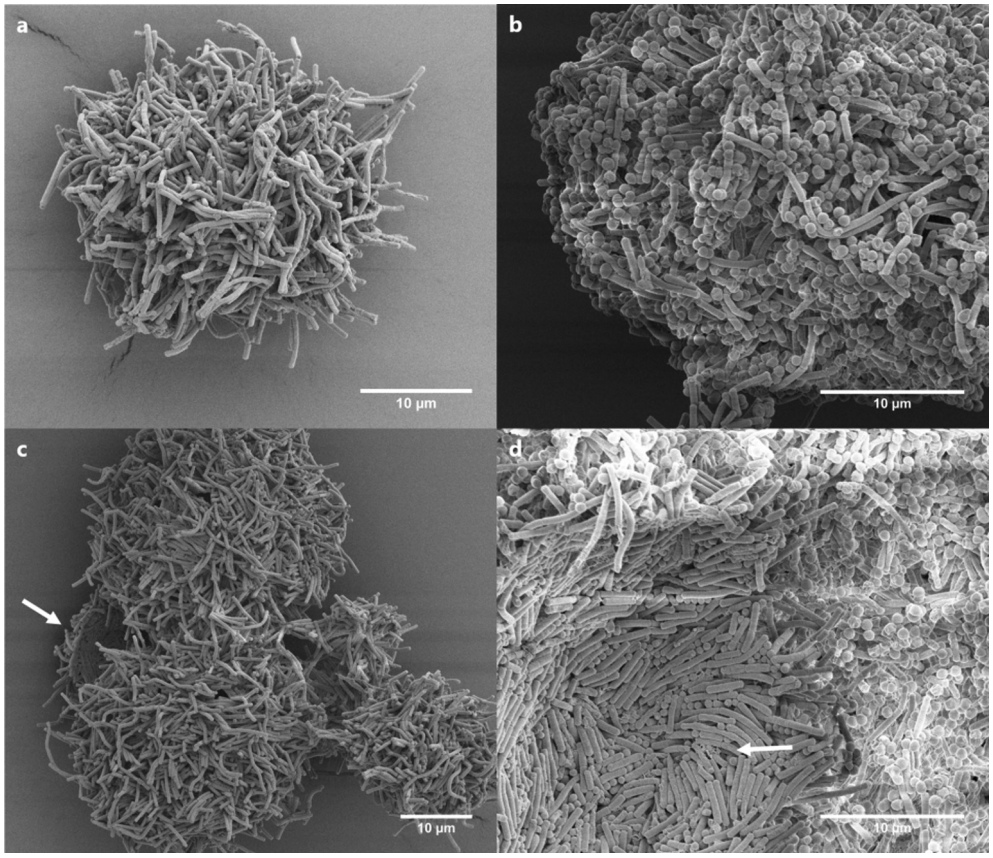

Fig. 6. LBC-CH-DS-CH colloidosome (a, c) and LBC-CH-PCP-CH colloidosome (b, d). The outer surface of the LBC-CH-DS-CH colloidosomes appeared hairy (a) due to the random packing of innermost LBC on the original air–water interface. (b) The adsorption of round-shaped PCP cells filled up some spaces of the hairy surface. Ruptured colloidosomes of polymer coating (c) and hybrid coating (d) formulations exposed a rather smooth inner surface and random packing of the innermost LBC. Scale bars represent 10 μm.

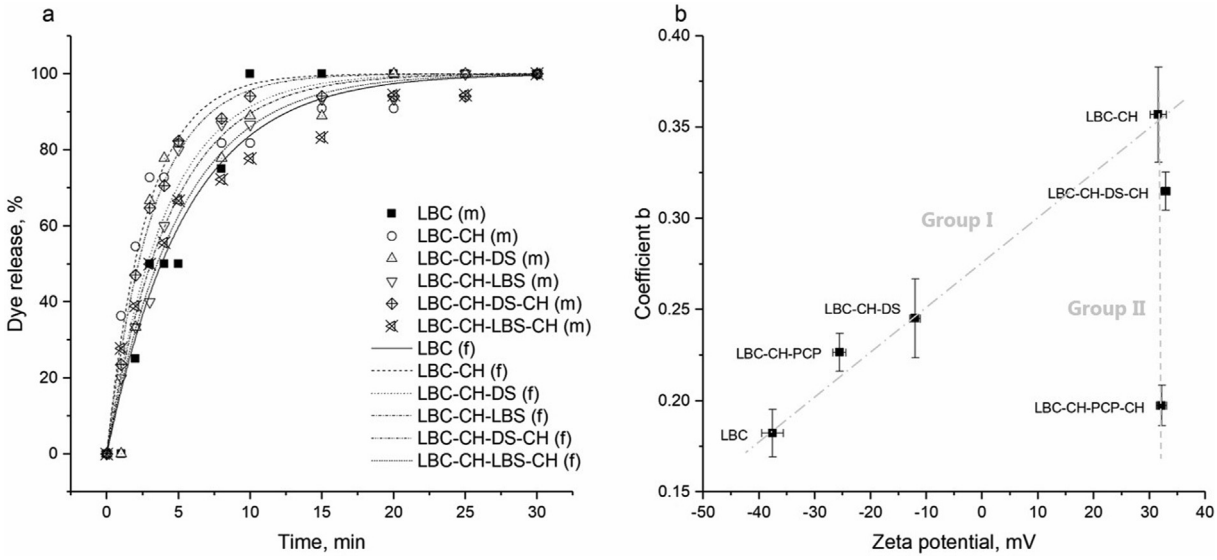

Fig. 7. Dye release (symbols) and model fit (lines) of different formulations of colloidosomes (a). Correlation between the parameter *b* representing permeability and the zeta potential of colloidosomes (b). Error bars represent the standard errors. The grey dash lines referring to group I and II are only to guide the eyes and are not based on regression.

that electrostatic repulsions between the anionic dye and colloidosomes was the most important permeation barrier for this group. Group II, constituting LBC-CH, LBC-CH-DS-CH and LBC-CH-PCP-CH colloidosomes that were finished with CH coating, all showed a zeta potential of about + 32 mV. In this cationic group, colloidosomes coated with three layers of polymers showed lower permeability than colloidosomes formed with only a layer of CH but higher permeability than colloidosomes formulated with a three-

layer hybrid combination involving PCP bacteria. For these colloidosomes with the absence of electrostatic repulsion, the permeability was predominantly controlled by the number of layers, wall thickness and the shell porosity. Therefore, the overall dye release behavior of colloidosomes seemed to be an interplay of both electrostatic effects and shell porosity. Based on this, different types and numbers of depositing layers can be employed to finely tune the shell permeability towards different encapsulated compounds with known sizes and charge densities.

4. Conclusions

The ability of lactic acid bacteria to strongly adsorb and aggregate at air–water interface was enhanced by surface chemical modification using OSA. The modified bacteria were capable of producing and stabilizing microbubble templates via fast locking themselves forming solid bacterial shells, which allowed the eventual displacement of air core by water core without structural disintegration. The microbubble-templated colloidosomes were further strengthened by LBL adsorption using either a polymer or hybrid coating formulation. Hollow structures were confirmed for all the colloidosomes and the outer surface was found hairy and porous due to the random packing of the innermost rod-shaped LBC. Hybrid coating involving round-shaped PCP cells achieved the artificial assembly of two bacterial species, which also resulted in a lower shell porosity than polymer coating due to the filling up of inner interstices by PCP cells. The permeability of colloidosomes was not solely dependent on the shell porosity, instead, the electrostatic repulsions between shells and the encapsulated compound played a key role especially when using medium of low ionic strength.

The fabrication of colloidosomes has been extensively reported to template on a liquid-core emulsion, where additional procedures such as centrifugation [20] or oil extraction [48] are needed to achieve complete removal of oil–water interface. Here we employed microbubbles as templates, which mitigates the use of these extra steps and lowers the risk of deconstructing the formed shell by reducing the mechanical or chemical stresses. Notably, this is the first work to prepare colloidosomes using solely microorganism cells with the ability to adsorb and aggregate at air–water interface, and subsequently applying hybrid coating combining polymers and living bacterial cells, as well as to artificially combine multiple microorganisms together into an organized structure. The tunable shell permeability of such structures provides potentials for encapsulation and controlled release of compounds. More interestingly, future studies could even incorporate more layers of different bacterial species and provide nutrients continuously while monitoring the growth of bacteria. In this way, a long-term symbiotic relationship may be constructed among multiple species of bacteria, which opens possibilities to apply the grown structures in, for example, the development of relevant biofilms.

CRediT authorship contribution statement

Xiaoyi Jiang: Conceptualization, Investigation, Methodology, Formal analysis, Writing – original draft. **Helle Jakobe Martens:** Investigation, Methodology, Writing – review & editing. **Elhamalsadat Shekarforoush:** Methodology, Writing – review & editing. **Musemma Kedir Muhammed:** Methodology, Writing – review & editing. **Kathryn A. Whitehead:** Writing – review & editing. **Nils Arneborg:** Writing – review & editing, Supervision. **Jens Risbo:** Conceptualization, Writing – review & editing, Supervision, Funding acquisition.

Declaration of Competing Interest

The authors declare that they have no known competing financial interests or personal relationships that could have appeared to influence the work reported in this paper.

Acknowledgements

The research leading to these results has received funding from The Danish Independent Research Foundation under framework grant n○ 8022-00139B and financial support of Chinese Scholarship Council (CSC) grant n○ 201807940009. Imaging data were collected at the Center for Advanced Bioimaging (CAB) Denmark, University of Copenhagen.

Appendix A. Supplementary material

Supplementary data to this article can be found online at https://doi.org/10.1016/j.jcis.2022.04.136.

References

[1] J.W. Kim, A. Fernández-Nieves, N. Dan, A.S. Utada, M. Marquez, D.A. Weitz, Colloidal assembly route for responsive colloidosomes with tunable permeability, Nano Lett. 7 (2007) 2876–2880, https://doi.org/10.1021/nl0715948.
[2] K.L. Thompson, M. Williams, S.P. Armes, Colloidosomes: Synthesis, properties and applications, J. Colloid Interface Sci. 447 (2014) 217–228, https://doi.org/10.1016/j.jcis.2014.11.058.
[3] F.J. Rossier-Miranda, K. Schroën, R. Boom, Microcapsule production by an hybrid colloidosome-layer-by-layer technique, Food Hydrocoll. 27 (2012) 119–125, https://doi.org/10.1016/j.foodhyd.2011.08.007.
[4] S. Lam, K.P. Velikov, O.D. Velev, Pickering stabilization of foams and emulsions with particles of biological origin, Curr. Opin. Colloid Interface Sci. 19 (2014) 490–500, https://doi.org/10.1016/j.cocis.2014.07.003.
[5] J. Li, H.D.H. Stöver, Pickering emulsion templated layer-by-layer assembly for making microcapsules, Langmuir 26 (2010) 15554–15560, https://doi.org/10.1021/la1020498.
[6] Y. Zhao, N. Dan, Y. Pan, N. Nitin, R.V. Tikekar, Enhancing the barrier properties of colloidosomes using silica nanoparticle aggregates, J. Food Eng. 118 (2013) 421–425, https://doi.org/10.1016/j.jfoodeng.2013.04.030.
[7] B.P. Binks, S.O. Lumsdon, Stability of oil-in-water emulsions stabilised by silica particles, Phys. Chem. Chem. Phys. 1 (1999) 3007–3016, https://doi.org/10.1039/A902209K.
[8] H.N. Yow, A.F. Routh, Release profiles of encapsulated actives from colloidosomes sintered for various durations, Langmuir 25 (2009) 159–166, https://doi.org/10.1021/la802711y.
[9] L.M. Croll, H.D.H. Sto, Formation of Tectocapsules by Assembly and Cross-linking of Poly (divinylbenzene- alt -maleic anhydride) Spheres at the Oil - Water Interface, Langmuir 55 (2003) 5918–5922, https://doi.org/10.1021/la026485h.
[10] S. Laïb, A.F. Routh, Fabrication of colloidosomes at low temperature for the encapsulation of thermally sensitive compounds, J. Colloid Interface Sci. 317 (2008) 121–129, https://doi.org/10.1016/j.jcis.2007.09.019.
[11] M.F. Hsu, M.G. Nikolaides, A.D. Dinsmore, A.R. Bausch, V.D. Gordon, X. Chen, J. W. Hutchinson, D.A. Weitz, Self-assembled Shells Composed of Colloidal Particles : Fabrication and Characterization, Langmuir 21 (2005) 2963–2970, https://doi.org/10.1021/la0472394.
[12] K.L. Thompson, S.P. Armes, J.R. Howse, S. Ebbens, I. Ahmad, J.H. Zaidi, D.W. York, J.A. Burdis, Covalently cross-linked colloidosomes, Macromolecules 43 (2010) 10466–10474, https://doi.org/10.1021/ma102499k.
[13] P. Arumugam, D. Patra, B. Samanta, S.S. Agasti, C. Subramani, V.M. Rotello, Self-Assembly and Cross-linking of FePt Nanoparticles at Planar and Colloidal Liquid - Liquid Interfaces, J. Am. Chem. Soc. 130 (2008) 10046–10047, https://doi.org/10.1021/ja802178s.
[14] S.A.F. Bon, S. Cauvin, P.J. Colver, Colloidosomes as micron-sized polymerisation vessels to create supracolloidal interpenetrating polymer network reinforced capsules, Soft Matter 3 (2) (2007) 194–199.
[15] Y. Chen, C. Wang, J. Chen, X. Liu, Z. Tong, Growth of Lightly Crosslinked PHEMA Brushes and Capsule Formation Using Pickering Emulsion Interface-Initiated ATRP, J. Polym. Sci. Part A Polym. Chem. 47 (2009) 1354–1367, https://doi.org/10.1002/pola.
[16] V.D. Gordon, X. Chen, J.W. Hutchinson, A.R. Bausch, M. Marquez, D.A. Weitz, Self-assembled polymer membrane capsules inflated by osmotic pressure, J. Am. Chem. Soc. 126 (2004) 14117–14122, https://doi.org/10.1021/ja0474749.
[17] M. Williams, S.P. Armes, D.W. York, Clay-based colloidosomes, Langmuir 28 (2012) 1142–1148, https://doi.org/10.1021/la2046405.

[18] F. Caruso, R.A. Caruso, H. Mőhwald, Nanoengineering of Inorganic and Hybrid Hollow Spheres by Colloidal Templating, Science 282 (5391) (1998) 1111–1114.
[19] F. Caruso, R.A. Caruso, H. Möhwald, Production of hollow microspheres from nanostructured composite particles, Chem. Mater. 11 (1999) 3309–3314, https://doi.org/10.1021/cm991083p.
[20] A.D. Dinsmore, M.F. Hsu, M.G. Nikolaides, M. Marquez, A.R. Bausch, D.A. Weitz, Colloidosomes: Selectively Permeable Capsules Composed of Colloidal Particles, Science 298 (5595) (2002) 1006–1009.
[21] Q. Sun, Z. Zhao, E.A.H. Hall, A.F. Routh, Metal coated colloidosomes as carriers for an antibiotic, Front. Chem. 6 (2018) 1–8, https://doi.org/10.3389/fchem.2018.00196.
[22] M.-P. Chapot-Chartier, S. Kulakauskas, Cell wall structure and function in lactic acid bacteria, Microb. Cell Fact. 13 (Suppl 1) (2014) S9, https://doi.org/10.1186/1475-2859-13-S1-S9.
[23] P. Schär-Zammaretti, J. Ubbink, The Cell Wall of Lactic Acid Bacteria : Surface Constituents and Macromolecular Conformations, Biophys. J. 85 (2003) 4076–4092, https://doi.org/10.1016/S0006-3495(03)74820-6.
[24] T.A. Camesano, B.E. Logan, Probing bacterial electrosteric interactions using atomic force microscopy, Environ. Sci. Technol. 34 (2000) 3354–3362, https://doi.org/10.1021/es9913176.
[25] X. Jiang, C.Y. Falco, K.N. Dalby, H. Siegumfeldt, N. Arneborg, J. Risbo, Surface engineered bacteria as Pickering stabilizers for foams and emulsions, Food Hydrocoll. 89 (2019) 224–233, https://doi.org/10.1016/j.foodhyd.2018.10.044.
[26] X. Jiang, E. Shekarforoush, M.K. Muhammed, K. Whitehead, A.C. Simonsen, N. Arneborg, J. Risbo, Efficient chemical hydrophobization of lactic acid bacteria – One-step formation of double emulsion, Food Res. Int. 147 (2021), https://doi.org/10.1016/j.foodres.2021.110460 110460.
[27] M.L. Brandy, O.J. Cayre, R.F. Fakhrullin, O.D. Velev, V.N. Paunov, Directed assembly of yeast cells into living yeastosomes by microbubble templating, Soft Matter 6 (2010) 3494–3498, https://doi.org/10.1039/c0sm00003e.
[28] E. Li, R. Mira de Orduña, A rapid method for the determination of microbial biomass by dry weight using a moisture analyser with an infrared heating source and an analytical balance, Lett. Appl. Microbiol. 50 (2010) 283–288, https://doi.org/10.1111/j.1472-765X.2009.02789.x.
[29] H.J. Busscher, A.H. Weerkamp, H.C. van Der Mei, A.W. van Pelt, H.P. de Jong, J. Arends, Measurement of the surface free energy of bacterial cell surfaces and its relevance for adhesion, Appl. Environ. Microbiol. 48 (1984) 980–983, https://doi.org/10.1128/aem.48.5.980-983.1984.
[30] M. Polak-Berecka, A. Waśko, R. Paduch, T. Skrzypek, A. Sroka-Bartnicka, The effect of cell surface components on adhesion ability of Lactobacillus rhamnosus, Antonie Van Leeuwenhoek 106 (4) (2014) 751–762.
[31] R.B. Qaqish, M.M. Amiji, Synthesis of a fluorescent chitosan derivative and its application for the study of chitosan-mucin interactions, Carbohydr. Polym. 38 (1999) 99–107, https://doi.org/10.1016/S0144-8617(98)00109-X.
[32] S. Ata, Coalescence of bubbles covered by particles, Langmuir 24 (2008) 6085–6091, https://doi.org/10.1021/la800466x.
[33] C. Linke, S. Drusch, Pickering emulsions in foods - opportunities and limitations, Crit. Rev. Food Sci. Nutr. 58 (2018) 1971–1985, https://doi.org/10.1080/10408398.2017.1290578.
[34] K. Millsap, G. Reid, H.C. van der Mei, H.J. Busscher, Cluster analysis of genotypically characterized Lactobacillus species based on physicochemical cell surface properties and their relationship with adhesion to hexadecane, Can. J. Microbiol. 43 (1997) 284–291, https://doi.org/10.1139/m97-039.
[35] G. Reid, P.L. Cuperus, A.W. Bruce, H.C. van der Mei, L. Tomeczek, A.H. Khoury, H.J. Busscher, Comparison of contact angles and adhesion to hexadecane of urogenital, dairy, and poultry lactobacilli: Effect of serial culture passages, Appl. Environ. Microbiol. 58 (5) (1992) 1549–1553.
[36] M. Rayner, D. Marku, M. Eriksson, M. Sjöö, P. Dejmek, M. Wahlgren, Biomass-based particles for the formulation of Pickering type emulsions in food and topical applications, Colloids Surfaces A Physicochem. Eng. Asp. 458 (2014) 48–62, https://doi.org/10.1016/j.colsurfa.2014.03.053.
[37] B. Kos, J. Šušković, S. Vuković, M. Simpraga, J. Frece, S. Matošić, Adhesion and aggregation ability of probiotic strain Lactobacillus acidophilus M92, J. Appl. Microbiol. 94 (2003) 981–987, https://doi.org/10.1046/j.1365-2672.2003.01915.x.
[38] A. Jamburidze, A. Huerre, D. Baresch, V. Poulichet, M. De Corato, V. Garbin, Nanoparticle-Coated Microbubbles for Combined Ultrasound Imaging and Drug Delivery, Langmuir 35 (2019) 10087–10096, https://doi.org/10.1021/acs.langmuir.8b04008.
[39] K. Moran, A. Yeung, J. Masliyah, Measuring interfacial tensions of micrometer-sized droplets: A novel micromechanical technique, Langmuir 15 (1999) 8497–8504, https://doi.org/10.1021/la990363g.
[40] N. Taccoen, F. Lequeux, D.Z. Gunes, C.N. Baroud, Probing the mechanical strength of an armored bubble and its implication to particle-stabilized foams, Phys. Rev. X. 6 (2016) 1–11, https://doi.org/10.1103/PhysRevX.6.011010.
[41] Q. Lv, Z. Li, B. Li, M. Husein, D. Shi, C. Zhang, Wall slipping behavior of foam with nanoparticle-armored bubbles and its flow resistance factor in cracks, Sci. Rep. 7 (2017) 1–14, https://doi.org/10.1038/s41598-017-05441-7.
[42] C.P. Whitby, E.J. Wanless, Controlling Pickering Emulsion Destabilisation: A Route to Fabricating New Materials by Phase Inversion, Materials (Basel). 9 (2016) 626, https://doi.org/10.3390/ma9080626.
[43] E. Dickinson, Food colloids - An overview, Colloids Surf. 42 (1989) 191–204, https://doi.org/10.1016/0166-6622(89)80086-1.
[44] M. Matos, A. Marefati, G. Gutiérrez, M. Wahlgren, M. Rayner, K. Abe, Comparative emulsifying properties of octenyl succinic anhydride (OSA)-modified starch: Granular form vs dissolved state, PLoS ONE 11 (8) (2016) e0160140.
[45] R. Taghi-Kilani, L.L. Gyürék, P.J. Millard, G.R. Finch, M. Belosevic, Nucleic acid stains as indicators of Giardia muris viability following cyst inactivation, Int. J. Parasitol. 26 (1996) 637–646, https://doi.org/10.1016/0020-7519(96)00033-1.
[46] E. Uenishi, T. Shibasaki, H. Takahashi, C. Seki, H. Hamaguchi, T. Yasuda, M. Tatebe, Y. Oiso, T. Takenawa, S. Seino, Actin Dynamics Regulated by the Balance of Neuronal Wiskott-Aldrich Syndrome Protein (N-WASP) and Cofilin Activities Determines the Biphasic Response of Glucose-induced Insulin Secretion, J. Biol. Chem. 288 (2013) 25851–25864, https://doi.org/10.1074/jbc.M113.464420.
[47] S. Wang, Y. Xiong, Y. Wang, J. Chen, J. Yang, B. Sun, Evaluation of PLGA microspheres with triple regimen on long-term survival of vascularized composite allograft – an experimental study, Transpl. Int. 33 (4) (2020) 450–461.
[48] D. Lee, D.A. Weitz, Double emulsion-templated nanoparticle colloidosomes with selective permeability, Adv. Mater. 20 (2008) 3498–3503, https://doi.org/10.1002/adma.200800918.